

## Structural investigation of the pressure induced effects in liquid crystals

This article has been downloaded from IOPscience. Please scroll down to see the full text article.

2005 J. Phys.: Condens. Matter 17 S3155

(<http://iopscience.iop.org/0953-8984/17/40/019>)

View [the table of contents for this issue](#), or go to the [journal homepage](#) for more

Download details:

IP Address: 129.252.86.83

The article was downloaded on 28/05/2010 at 06:01

Please note that [terms and conditions apply](#).

# Structural investigation of the pressure induced effects in liquid crystals

L Noirez, G Pépy and P Baroni

Laboratoire Léon Brillouin (CEA-CNRS), CE-Saclay, 91191 Gif-sur-Yvette Cédex, France

E-mail: [noirez@llb.saclay.cea.fr](mailto:noirez@llb.saclay.cea.fr)

Received 8 July 2005

Published 23 September 2005

Online at [stacks.iop.org/JPhysCM/17/S3155](http://stacks.iop.org/JPhysCM/17/S3155)

## Abstract

Liquid crystal phases are characterized by a long range orientational order. Numerous studies on liquid crystals under hydrostatic pressure display interesting pressure induced phenomena which seem to indicate that this long range order is disturbed. It is shown for example that re-entrant phases appear and that phase transition temperature shifts are commonly observed. These pressure induced effects result from the packing properties exacerbated by the pressure induction of the molar volume.

Despite numerous developments, the structural modifications which accompany these pressure induced effects, as the phase transition temperature shifts, have hardly been investigated. We provide, using neutron diffraction, the physical reasons for these temperature shifts. We report here on the very few structural studies of the influence of hydrostatic pressure on the stability of a liquid crystal phase. This study is carried out using two specifically designed neutron pressure cells reaching pressure values up to 120 MPa. The liquid crystal system is described in terms of pressure-induced correlation lengths and layer spacing, which are the relevant parameters to account for the phase structure. It will be shown that the structural investigation is particularly noteworthy in the lamella phase since the characteristic lengths can be tremendously modified under pressure, underlining a correlated change of dynamics. In the case of high molecular weight liquid crystals (side-liquid crystal polymers), it will be shown that the re-entrant nematic–smectic transition is unchanged with respect to the pressure, indicating that the pressure induced reduction of the specific volume concerns the polymer component only.

(Some figures in this article are in colour only in the electronic version)

## 1. Introduction

The observation of the influence of a hydrostatic pressure on the phase transition temperatures of liquid crystals is almost as ancient as the discovery of the liquid crystallinity. The first

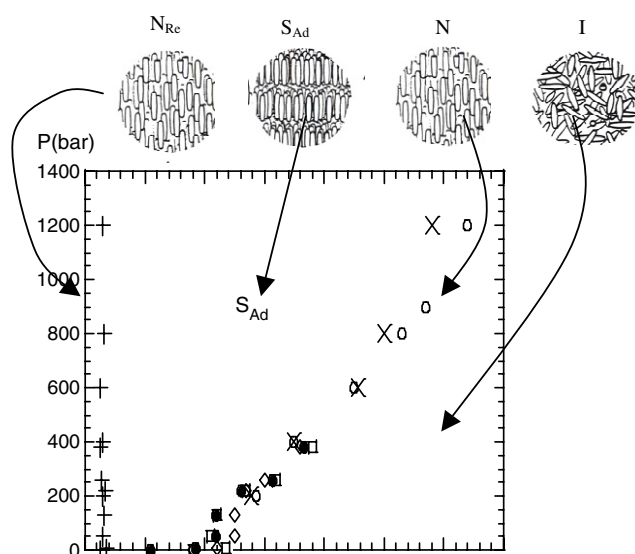


**Figure 1.** Organization of the liquid crystal phases (isotropic, nematic, smectic) and Clapeyron diagram corresponding to the molecule studied (from [5]).

Clapeyron diagram is due to Hulett in 1899, who made the first visual observations of phase transition changes through a capillary tube, applying increasing hydrostatic pressure until the tube broke (30 MPa) [1].

The study of the properties of thermotropic liquid crystals was then considerably extended in the 1970s, benefiting from the emergence of various techniques of characterization (optical transmission, DSC, NMR, x-rays, volumetry, Raman, refractive index. . .). In the conventional description, the isotropic phase is the high temperature state corresponding to a liquid-like state in which the liquid crystal molecules, that are rod shaped, are randomly distributed. By decreasing the temperature, a nematic phase generally succeeds; this liquid crystalline phase is characterized by a long range orientational order. Finally, at lower temperature, the smectic phase appears. Figure 1 displays from right to left the scheme of the structure of the isotropic, the nematic and the smectic phases. In addition to the orientational order, the smectic phase possesses a positional order in layers. It is demonstrated that the isotropic–nematic and the nematic–smectic phase transitions are separated by (weakly) first order transitions [2]. Concerning the pressure induced effects, most remarkable phase diagrams listed in the literature report on the occurrence of tricritical points, which indicate the appearance of pressure induced liquid crystallinity in compounds purely crystalline at atmospheric pressure [3]. It has been also established that pressure produces antagonist effects [4]; it can reinforce the ordering of the mesophase (increase of the order parameter) and reveal symmetries frustrated at atmospheric pressure or it can destabilize the molecular interactions which give rise to the long range liquid crystal order, destroying the liquid crystal properties. These examples show that the liquid crystal is a fragile assembly. In contrast to solid-state crystals, the liquid crystal symmetry does not result from the repetition of an elementary unit, but from the establishment of an order at long range, whereas locally the molecular dynamics is liquid-like. These fundamental differences point out the strong sensitivity of liquid crystals to low pressures and the richness of the pressure–temperature phase diagrams.

Pressure induced effects as the temperature shifts or changes of phase symmetry are established for a broad category of liquid crystal molecules [4]. There are in contrast, to our

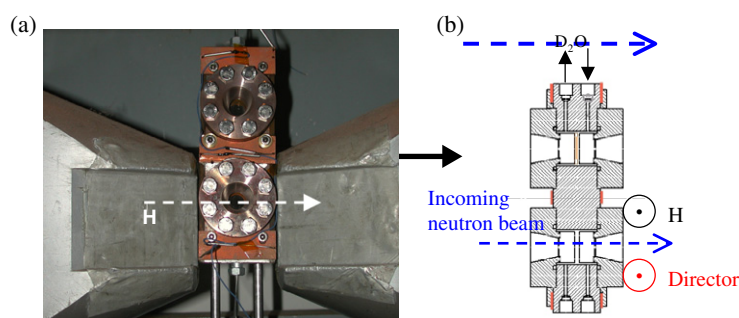


**Figure 2.** Photograph of the double-sample-holder pressure cell, placed between the poles of a horizontal magnetic field of 1.5 T. The distance between the two poles is 52 mm and the arrow represents the direction of the magnetic field.

knowledge, very few structural descriptions illustrating the pressure effects on the structural parameters characterizing the long range liquid crystal order.

Here, we present one of the first neutron diffraction studies on pressure effects on liquid crystal structures. We will focus on the pressure induced effects within the smectic phase (figure 1(c)). The aim is to correlate the temperature–pressure smectic phase diagram to structural modifications [5]. The relevant parameters are the following:

- the interlayer distance within the smectic phase;
- the smectic order parameter, which indicates the density of the liquid crystal molecules;
- the longitudinal and transverse correlation lengths ( $\xi_{\parallel}$ ,  $\xi_{\perp}$ ). These values measure the range of extension of the smectic order along and perpendicular to the director respectively. The smectic order is limited because of its dynamical distortions, inherent to a two-dimensional plane (Landau–Peierls instabilities).

In the frame of this study, we had to elaborate a new pressure cell specially devoted to neutron scattering, presenting a high transmission power with respect to the wavelength range, abmagnetic to allow the orientation of the liquid crystal using a magnetic field. Finally, its optical transparency allows a direct visual control of the sample state and optionally the measurement of the evolution of the birefringence under pressure.

## 2. Description of the pressure cell: the technical challenge

The pressure cell (figures 2(a) and (b)) has been built to resist to pressures up to 200 MPa, to reach temperatures up to 150 °C, to be transparent with respect to neutron wavelengths and to allow the orientation of the samples using an external magnetic field.

The clamping discs of the cell are made of a non-magnetic material, a beryllium–copper alloy (ST25 from the Stainless Company). The in and out beam windows are made of synthetic sapphire discs of 20 mm diameter and 10 mm thickness, whereas the sample thickness is 1 mm. The pressure transmitting fluid is also transparent optically and to neutron scattering:  $D_2O$ . The watertightness of the pressure chamber is ensured using O-ring seals (Advanced Products) between the clamping discs and the main cell alloy body. Figure 2(a) shows the pressure cell *in situ* installed between the poles of a magnet. The cell contains a second sample chamber. This lodgement has been built to allow specific volume differential measurements with a reference sample. Finally, these experiments have also needed the development of an original technique of sample encapsulation [6]. The sample is mounted in the molten state, under vacuum, in a

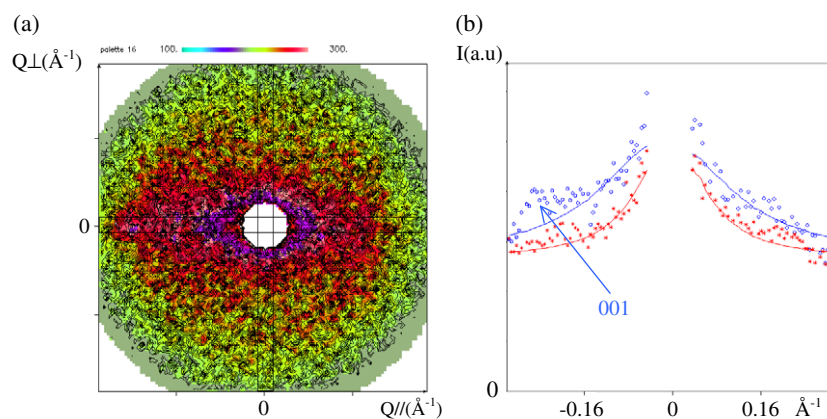
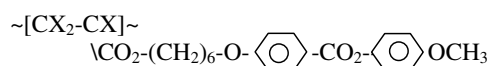


**Figure 3.** (a) Small angle two-dimensional scattering pattern produced by a smectic liquid–crystal polymer under pressure ( $p = 40$  MPa) aligned under magnetic field (mixture of hydrogenated and deuterated polymers). The scattering conditions were  $\lambda = 10$  Å and a detector–sample distance of 1.5 m (PAXY spectrometer, LLB, Orphée Reactor). The chemical formula of the sample is:



where X = H or D. The molecular weight of the H/D mixture is  $26\,000$  g mol $^{-1}$  and the polydispersity about 2.6. (b) Corresponding profiles of the scattering curves along and perpendicular to the phase director. The continuous lines correspond to the Lorentzian fits (the red and the blue lines correspond to the perpendicular and the parallel fits respectively) of the polymer form factor. The smectic reflection can be identified at  $Q \approx -0.25$  Å $^{-1}$ .

cuvette formed by a quartz disc and a ring. A thin Kapton film is glued on the ring and covers the sample. The suppleness of this membrane ensures the transmission of the pressure to the sample.

In addition to diffraction measurements, the high transmission power and the low scattering of the sapphire windows allow us to extend the use of the pressure cell to small angle neutron scattering (SANS) range measurements. This scattering technique associated with a partial labelling remains the only method to date adapted to determine the bulk polymer conformation [7]. The signal associated with this contrast method is often weak. As a result, SANS measurements are possible only if the background noise is sufficiently reduced (this type of measurement is not possible when the pressure-cell windows are made of metallic material). The present pressure cell is performing for such low intensity measurements. Figure 3 illustrates the neutron scattering pattern obtained with the pressure cell, which displays the form factor of the main chain of a smectic LC-polymer. The signal is elongated along the horizontal axis, which means that the polymer chains are elongated perpendicularly to the phase director axis. Quantitatively, such an anisotropic form factor can be modelled with a 2D Lorentzian function (figure 1(a)). The anisotropy rate between the chain dimensions along and perpendicular to the director is estimated at about two. The impact of a hydrostatic pressure on the conformational properties of different polymer systems is under way and will be detailed in a future paper specially devoted to a conformational behaviour.

### 3. Experimental details

To examine the stability of the smectic phase with respect to the pressure, we use the neutron diffraction properties. This phase is characterized by a two-dimensional order which gives

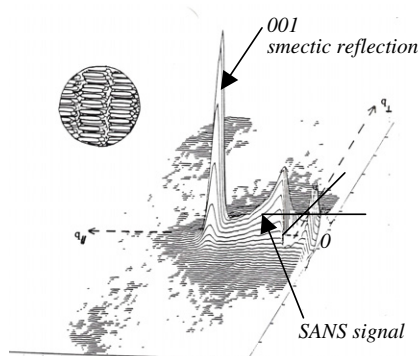


**Figure 4.** Two-dimensional scattering pattern at larger scattering angle (diffraction conditions) displaying the 001 smectic reflection of a liquid crystal polymer.

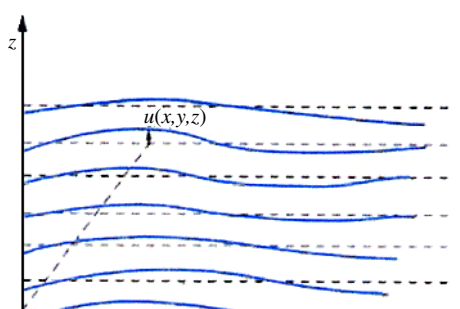


**Figure 5.** Representation of the lamella phase (smectic phase) and of the associated 2D instabilities (Landau–Peierls instabilities).

rise in the reciprocal space to smectic reflections, well accessible by diffraction techniques (figure 4). From a thermodynamic point of view, such a 2D arrangement is unstable and gives rise to layer undulations. This instability has been theoretically described by Landau and Peierls (figure 5) [8]. The free energy  $F$  contains two terms  $B$  and  $K$  that describe the elastic constants of compression and of curvature respectively.  $B$  corresponds to an energy per volume unit (of about  $10^5 \text{ J m}^{-3}$ ) whereas the curvature constant  $K$  has the dimension of a force and displays values of about  $10^{-12} \text{ N}$  [9].

$$F = F_0 + \frac{1}{2}B(du/dz)^2 + \frac{1}{2}K(d^2u/dx^2 + d^2u/dy^2)^2$$

where  $u$  is the layer displacement.

The effects of the layer undulation dynamics are visible in the diffraction reflection profiles. Indeed, the widths of the smectic reflections are larger than in a crystal. The intensity of the first Bragg peak position being much larger than the higher orders, the system is usually described considering the evolution of the first order only as relevant [2].

The scattering intensity of the 001 order decreases from a maximum  $I_0$  following a power law:  $I(q_{001}) = I_0/|q_{001} - q|^2^{-\eta}$ , where  $\eta$  is an exponent depending on the temperature and on the elastic constants [8] and  $q$  the scattering vector.

From a practical point of view, the samples are placed in the molten state between two quartz discs sealed by a 1 mm thickness ring of 22 mm diameter. The sample (1 mm thickness) is macroscopically aligned by decreasing the temperature from the isotropic phase down to

the smectic phase under the continuous magnetic field of 1.2 T. The magnetic field acts on the diamagnetic properties of the liquid crystalline molecule (the biphenyl part), provoking a torque on each molecule (Lenz law). The liquid crystal molecules are gathered in monodomains defined by the volume occupied by the molecular set presenting a common orientation, they have a length scale of the order of some microns. Under magnetic field, the addition of the elementary diamagnetic torques produces a macroscopic torque at the scale of each monodomain ( $\mu\text{m}$  scale) which reorients these liquid crystal polydomains in one monodomain oriented along the direction of the magnetic field. The following discussion concerns only results obtained on monodomain samples.

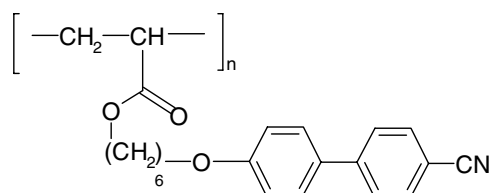
From a scattering point of view, we consider essentially the 001 smectic reflection (the higher orders being much weaker). We determine quantitatively the widths at half maximum  $\xi_i$  of the intensity curve. The intensity reflection is approximated to a Gaussian variation and deconvoluted from the device resolution (Rietveld approximation):  $I = I_0 \exp(-[(q - q_0)^2/\Delta q_{\parallel}^2 + q_{\perp}^2/\Delta q_{\perp}^2]16/\ln 2^2)$ , where the symbols  $\parallel$  and  $\perp$  indicate the directions parallel and perpendicular to the magnetic field respectively. The widths  $\Delta q_{\parallel}$  and  $\Delta q_{\perp}$  are related to the respective correlation lengths  $\xi_{\parallel}$  and  $\xi_{\perp}$  via  $\xi_i = 4\pi/\Delta q_i$ . These parameters are measured as a function of the temperature on an aligned liquid crystal domain by increasing pressure from atmospheric pressure up to 120 MPa. The experimental set-up used in this experiment is the two-axis spectrometer (3T1) of the Laboratoire Léon Brillouin (CEA-CNRS). The wavelength was 2.36 Å with a standard collimation and without analyser (the liquid crystal dynamics is too slow to produce an inelastic contribution). Finally, longitudinal and transverse scans are systematically carried out at each measurement.

#### 4. Sample

The sample used is a high molecular weight liquid crystal of side-chain polymer type. It consists in grafting liquid crystal moieties regularly onto the side of an ordinary chain (usually by esterification as shown in the following chemical sample) [10].

These polymeric side-chain liquid crystals possess static properties similar to the conventional low molecular weight homologues. Their mesomorphic properties are indeed entirely due to the liquid crystal moieties. Similarly to every polymer material, these systems are moulded, extruded, injected, . . . All these technical processes involve various stresses among which the pressure plays an important role. It is therefore particularly useful to determine the impact of an hydrostatic pressure on the phase properties of these polymers.

We will devote our study to the polymer liquid crystal described in [11]. The main-chain is a polyacrylate chain. The mesomorphic part is a cyano-biphenyl group grafted onto the chain via an alkyl spacer of six carbons:



It displays the following phase sequence including a nematic re-entrance:  $T_g-35^\circ\text{C}-\text{N}_{\text{Re}}-83^\circ\text{C}-\text{S}_{\text{Ad}}-110^\circ\text{C}-\text{N}-122^\circ\text{C}-\text{I}$  (transition temperatures determined by DSC and microscopy), where 'I' stands for isotropic, 'N' for nematic, 'S<sub>Ad</sub>' for smectic and 'N<sub>Re</sub>' for re-entrant nematic phase.



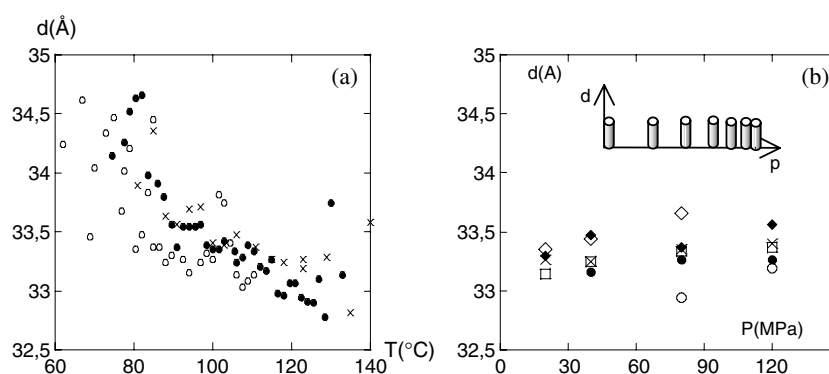


**Figure 6.** (a) Evolution of the smectic layer thickness as a function of the temperature at various pressures:  $\circ$ , 40 MPa;  $\times$ , 80 MPa;  $\bullet$ , 120 MPa. (b) Layer thickness versus pressure at  $T = 100^\circ\text{C}$ . The inset gives a scheme of the pressure induced reduction of the lateral spacing between rod-like liquid crystal molecules. Diffraction measurements are carried out on spectrometer 3T1 of the LLB.

## 5. Results and discussion

### 5.1. Influence of the pressure on the layer distance

Figure 6(a) displays the evolution of the smectic layer distance  $d$  at different pressures versus temperature. The effect due to the temperature variation is stronger than the pressure influence. It can be considered that the smectic layers are almost incompressible in this pressure range. The reduction of the layer thickness with increasing temperature is conventionally explained by the decrease of the order parameter and thus an isotropization, and thus a reduction along the director of the anisotropic dynamic volume described by the rod-like mesogen.

The increasing pressure implies a correlative decrease of the specific volume. Since the layer distance is invariant, the specific volume is anisotropically reduced; only the inter-(lateral) molecular distance is reduced. This pressure induced transition from low density to high density smectic phase is illustrated at the bottom of figure 6(b). It also results correlatively in a restriction of the amplitude of the lateral mobility, implying a modification of the elastic constant of curvature  $K$  towards an increase of the layer rigidity.

### 5.2. Influence of the pressure on the smectic order parameter

The diffracted intensity is proportional to the square of the order parameter of the smectic phase  $\psi_0$  [2]. Indeed, neglecting higher orders of reflections, the smectic phase can simply be represented as a sinusoidal modulation of the scattering length density  $\psi(z) = \psi_0 \sin(z2\pi/d)$  where  $d$  is the layer period and  $z$  the coordinate along the director axis.  $\psi_0$  is calculated from  $\sqrt{I_0}$ . It measures the number of molecules localized in the layer. Figure 7(a) displays the variation of the order parameter as a function of the temperature at different pressure values.  $\psi_0$  is strongly dependent on the pressure, but its variation is not linear. Figure 7(b) illustrates the evolution of the order parameter versus pressure at  $T = 110^\circ\text{C}$ . The evolution is rapid from atmospheric pressure up to 40–60 MPa and then a maximum seems to be reached from 60 MPa. From atmospheric pressure up to 40–60 MPa, the packing of the liquid crystal molecules into the layer increases ( $\psi_0$  increases). This increase of the smectic order parameter provokes correlatively an increase of the layer rigidity. From 60 up to 120 MPa, the order parameter does not evolve anymore. The absence of further variation can be interpreted as a



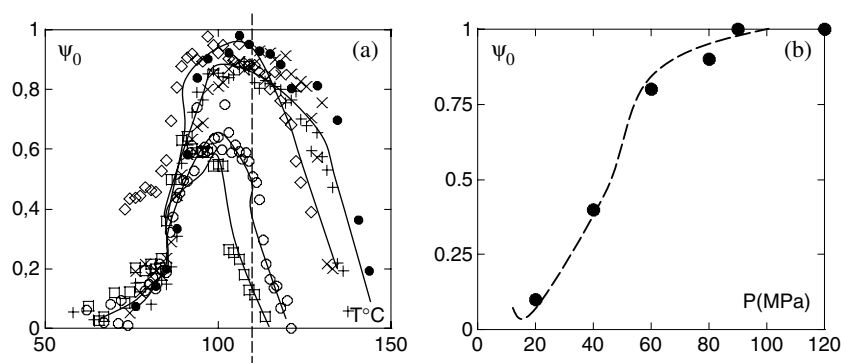


**Figure 7.** Evolution of the smectic order parameter  $\psi$  versus temperature at different pressures:  $\square$ , 20 MPa;  $\circ$ , 40 MPa;  $\diamond$ , 60 MPa;  $\times$ , 80 MPa;  $+$ , 90 MPa;  $\bullet$ , 120 MPa.

maximum in the pressure induced packing. Let us take  $\psi_0 = 1$  when  $\psi_0$  has reached its highest value. Figure 7(a) also reveals an asymmetry of the evolution of the two transitions  $N_{\text{Re}}-S_{\text{A}}$  and  $S_{\text{A}}-N$  versus pressure. The  $N_{\text{Re}}-S_{\text{A}}$  transition is relatively insensitive to the pressure whereas the  $S_{\text{A}}-N$  transition is strongly pressure dependent. This shows that the mechanisms involved in both transitions are different. The  $N_{\text{Re}}-S_{\text{A}}$  is related to local attractive polar-polar intermolecular transition [12, 13]; the medium pressures applied here are not sufficient to modify the corresponding dynamics. In contrast, the  $S_{\text{A}}-N$  transition is conditioned by the stability of the pretransitional smectic fluctuations, which are established at long range, i.e. weak molecular interactions. These are thus more sensitive to a macroscopic stress. The pressure induced condensation of the pretransitional smectic fluctuations into a long range smectic order corresponds to the transition from the nematic symmetry to the higher symmetry smectic phase; the smectic phase is thus extended by increasing the pressure towards higher temperatures.

### 5.3. Influence of the pressure on the smectic phase correlation lengths

The effect of the pressure on the correlation lengths  $\xi_{\parallel}$  and  $\xi_{\perp}$  is displayed in figures 8(a) and (b). As expected, both correlation lengths are enhanced under pressure. Since the layer undulation is the main parameter limiting the correlation length, it can be concluded that the layer distortion is strongly reduced under pressure; the order range is consequently more extended. Both parameters evolve similarly, meaning that there is a direct relationship between  $\xi_{\parallel}$  and  $\xi_{\perp}$ . These quantities are indeed linked to the previously defined elastic constants  $B$  and  $K$ ; these values depend on the order parameter [14]. These features are thus coherent with the evolution of the order parameter. The pressure favours the parallelism of the lamellae assembly. It can be noticed that whatever the pressure, the evolution of the correlation lengths with the temperature is not monotonic but passes through a maximum for each pressure. The correlation lengths increase by converting by increasing pressure more and more pretransitional smectic fluctuations into a long range smectic order. This conversion defines the upper temperature smectic phase limit. These values rapidly reach the limit of the device resolution (about 2500  $\text{\AA}$  in both directions). It is thus impossible to know if  $\xi_{\parallel}$  and  $\xi_{\perp}$  continue to evolve above 50–60 MPa. From an experimental point of view, the phase appears as a perfect 2D crystal since the mosaicity is higher than the standard resolution. Since the dynamical properties (undulation instabilities) of the high pressure induced phase are no longer measurable, the smectic phase can be considered as a frozen 2D state.

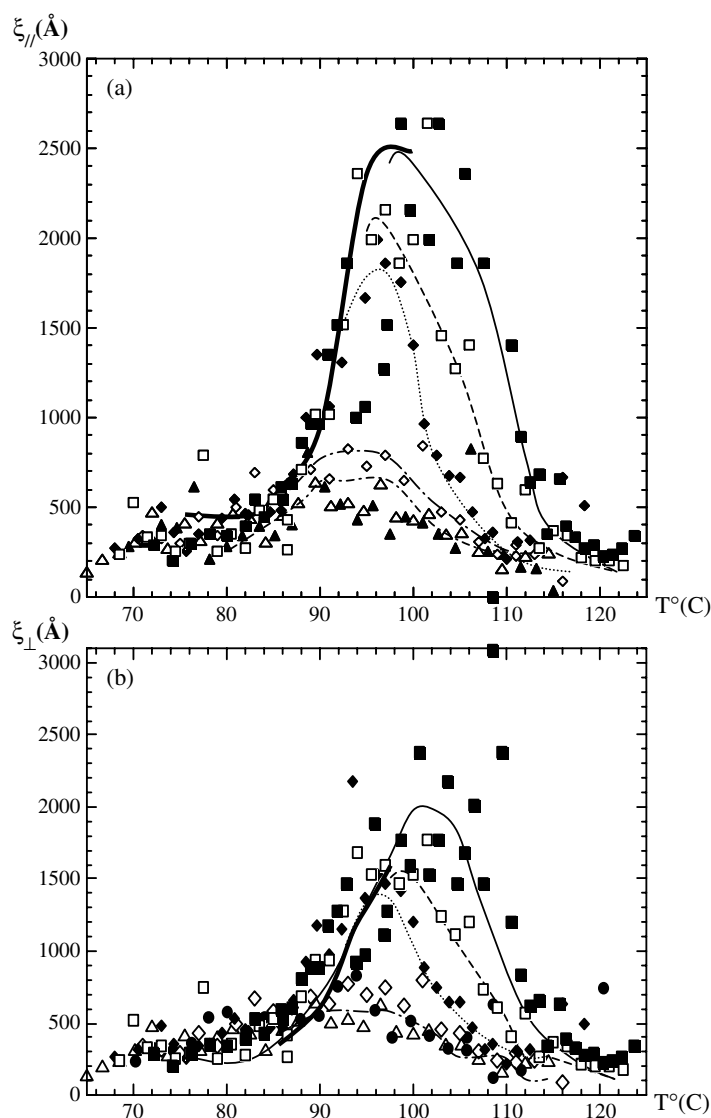


**Figure 8.** Evolution of the correlation lengths  $\xi_{||}$  and  $\xi_{\perp}$  as a function of the temperature at various pressures from atmospheric pressure up to 38 MPa (at this pressure and above, the limit of the spectrometer resolution is reached). (a) Along the director:  $\blacktriangle$ , 0.1 MPa;  $\triangle$ , 0.7 MPa;  $\diamond$ , 13 MPa;  $\blacklozenge$ , 22 MPa;  $\square$ , 26 MPa;  $\blacksquare$ , 38 MPa. (b) Perpendicular to the director:  $\blacktriangle$ , 0.1 MPa;  $\triangle$ , 0.7 MPa;  $\bullet$ , 5 MPa;  $\diamond$ , 13 MPa;  $\blacklozenge$ , 22 MPa;  $\square$ , 26 MPa;  $\blacksquare$ , 38 MPa.

## 6. Conclusions

We have reported here an overview of the possibilities offered by the technique of neutron scattering for the investigation of liquid crystal systems under extreme conditions. The very long mean free path of neutron scattering allows us to use heavy experimental environments as in the case of pressure experiments. Compared to conventional methods (x-rays), this is an important advantage. In the frame of the study of this thermotropic liquid crystal melt,

the following remarkable features can be drawn. The pressure acts by restricting the lateral space between mesogens in the smectic phase without modifying the layer spacing (within the 20–120 MPa pressure range). The pressure-induced free volume reduction embeds the 2D undulation of the layers (Landau–Peierls instability) and increases the longitudinal and transverse correlation ranges of the phase. Considering the resolution limitations of the spectrometer, above about 50–60 MPa, the pressure induced smectic phase appears as a perfect 2D crystal order.

Our set-up can be easily extended to both large and small angle scattering study of the pressure induced behaviour of various soft materials, in particular to solutions such as lyotropic systems since various structural transitions have been identified versus temperature and concentrations in these systems, which are still poorly understood.

## References

- [1] Hulett G A 1899 *Z. Phys. Chem.* **28** 629
- [2] de Gennes P G and Prost J 1993 *The Physics of Liquid Crystals* (Oxford: Oxford Science Publications)
- [3] Shashidar S and Chandrasekhar S 1975 *J. Physique Coll. IV* **36** C1 49
- [4] Cladis P E, Bogardus R K, Daniels W B and Taylor G N 1977 *Phys. Rev. Lett.* **39** 720  
McKee T J and Mc Coll J R 1972 *Phys. Rev. Lett.* **29** 85
- [5] Pépy G, Baroni P and Noirez L 2003 *Phys. Rev. E* **67** 41714
- [6] Baroni P and Pépy G 2002 *Rev. Sci. Instrum.* **73** 480
- [7] Higgins J S and Benoît H C 1994 *Polymers and Neutron Scattering* (Oxford: Oxford Science Publications)
- [8] Landau L and Lifschitz E 1967 *Physique Statistique* (Moscow: Mir)
- [9] Oswald P and Pieranski P 2002 *Les Cristaux-Liquides* Scientifiques edition (London: Gordon and Breach)  
Srivastava A and Singh S 2004 *J. Phys.: Condens. Matter* **16** 7169
- [10] Demus D, Goodby J, Gray G W, Spiess H W and Vill V (ed) 2000 *Handbook of Liquid Crystals* vol 3
- [11] Noirez L, Keller P, Davidson P, Hardouin F and Cotton J P 1988 *J. Physique* **49** 1993
- [12] Indeku J O and Becker A N 1986 *Phys. Rev. A* **33** 1158
- [13] Becker A N and Walker J S 1981 *Phys. Rev. Lett.* **47** 65
- [14] de Gennes P G 1973 *Mol. Cryst. Liq. Cryst.* **21** 49  
de Gennes P G 1972 *Solid State Commun.* **10** 753